J. Fluid Mech. (1992), *vol.* 234, *pp.* 613–627
Printed in Great Britain

The stability of three-dimensional time-periodic flows with spatially uniform strain rates

By A. D. D. CRAIK AND H. R. ALLEN
Department of Mathematical & Computational Sciences, University of St. Andrews, St. Andrews, Fife, KY16 9SS, Scotland

(Received 24 January 1991)

Unbounded incompressible fluid in solid-body rotation is subjected to spatially uniform strain rates that are sinusoidal in time and of arbitrarily large amplitude. The exact governing equations for the evolution of plane-wave disturbances to this time-periodic flow are linear, as for related steady flows. Attention focuses mainly on the inviscid problem, since incorporation of viscosity is straightforward.

Plane-wave disturbances to axisymmetric flows are governed by a Hill's equation, or equivalently, a pair of first-order equations, to which Floquet theory is applied. Analytical and computational results show several instability bands, the first few of which can exhibit large growth rates. The exact governing equations for plane-wave disturbances to non-axisymmetric flows are similarly derived; but, as these are not singly periodic, results are given only for small-amplitude periodic forcing. As the non-axisymmetric strain produces a periodic elliptical distortion of the flow, a modified elliptical-instability mechanism joins that present in axisymmetric cases.

Despite necessary idealizations, the analysis and results shed light on the stability of periodically strained vortices in a turbulent environment and in geophysical contexts.

1. Introduction

Solutions of the Navier–Stokes and Euler equations may be obtained, without approximation, for spatially periodic disturbances of arbitrarily large amplitude embedded in 'basic' shear flows with spatially uniform strain rates. The procedure is described by Craik & Criminale (1986) and further exploited in Craik (1988, 1989). Antecedents, limited to special cases and mostly based on linear approximation (which is unnecessarily restrictive), are referenced in these works: note particularly Kelvin (1887) and Lagnado, Phan-Thien & Leal (1984).

An important special case is that of two-dimensional flow with elliptical streamlines and constant vorticity: the instability observed in numerical simulations of Pierrehumbert (1986) motivated Bayly (1986) to examine this flow analytically, independently of Craik & Criminale (1986). Later studies followed, by Landman & Saffman (1987) and, with addition of Coriolis force, by Craik (1989). The realization that this flow is unstable, through a resonance mechanism, aroused considerable interest among workers on turbulence. For, the elliptical flow may be regarded as a local approximation of an eddy deformed by uniform external strain; and the instability provides a mechanism for spontaneous growth of wavenumbers small compared with the eddy size. Of course, disturbances of finite eddy structures must be affected by boundary conditions neglected in the unbounded case. But complementary theoretical and experimental work on stability of bounded elliptical

flows (the former, in contrast to the unbounded case, being restricted to linearized or Galerkin approximation) yield results that display essentially the same resonance instability mechanism: see Gledzer *et al.* (1975), Vladimirov (1983), Robinson & Saffman (1984), Malkus (1989), Waleffe (1990), and reviews by Craik (1991) and Gledzer & Ponomarev (1992).

The (unbounded) elliptical instability has also been invoked in explanation of the well-known secondary three-dimensional instability of laminar boundary layers (Landman & Saffman 1987; Bayly, Orszag & Herbert 1989). However, though distortion and stretching of vorticity hold the key to a physical understanding of both processes, the similarity between an unbounded vortex and a wall-bounded shear flow seems to us too remote to be helpful. Moreover, the usual explanation in terms of nonlinear interaction of two-dimensional and oblique Tollmien–Schlichting waves in boundary layers seems quite satisfactory (see for example Craik 1985).

Given that the unbounded elliptical instability provides an informative model of strained eddies in turbulence, it is worthwhile to elucidate other models that yield local approximations of turbulent flows. The work of Lagnado *et al.* (1984) on the linear stability of steady flows with hyperbolic streamlines may be so interpreted: stretching of disturbance vorticity (see also Pearson 1959; Craik & Criminale 1986) then yields rapid disturbance growth. However, for most initial disturbances, this is also associated with an exponential increase in wavenumber; and this continuous reduction in the lengthscale of disturbances means that inviscid growth is ultimately annihilated by viscous dissipation. (In contrast, the elliptical instability involved continuous net growth while the wavenumber varies periodically, and so is not ultimately dominated by viscous processes.) Nevertheless, the initial period of growth in hyperbolic flows may be crucially important, for it could lead to more complex flows through nonlinear mode interactions neglected in the single-mode formulation: for an example of such mode interaction in plane Couette flow, see the numerical simulation of Haynes (1987). Also, there are exceptional modes that are not ultimately damped: Craik & Criminale (1986, pp. 20, 24) drew attention to a mode with continuously decreasing wavenumber that has locally constant vorticity and so velocities that increase exponentially with the increasing lengthscale.

Here, we investigate the class of time-periodic basic flows with spatially uniform strain rates. These can be thought of as idealizations of local features within turbulent flows that display fluctuating rates of strain due to external excitation, either deliberately imposed at boundaries or caused by neighbouring 'eddies'. Such flows are amenable to analysis and clarify several important questions. In particular, (i) what range of wavenumbers is driven unstable by periodic excitation? (ii) does the instability of these time-periodic flows reveal any new physical mechanism, apart from the elliptic instability? (iii) do larger fluctuations of the basic flow necessarily lead to stronger instabilities, or is the disturbance growth rate limited by some detuning process?

Of course, the study of oscillatory forced systems has a long history, from Faraday (1831) onwards, but previous studies are restricted to linearized or weakly nonlinear approximations – see, for example, Benjamin & Ursell (1954), Nayfeh & Mook (1979), Miles & Henderson (1990). Closest in motivation to the present work (but employing linearized approximations) are the studies of McEwan & Robinson (1975) and Mansour & Lundgren (1990). The former investigate a density-stratified fluid in an oscillating container; but the well-known analogy between density-stratification and uniform rotation allows parallel conclusions to be drawn for rotating flows. The latter study a compressible flow in solid-body rotation that is subjected to weak

periodic compression and rarefaction along the axis of rotation. In both cases, a Mathieu or Hill's equation controls the linear stability of plane waves, as is also found here for axisymmetric flows.

After the general formulation of §2, §§3 and 4 focus on axisymmetric basic flows and §5 on non-axisymmetric ones.

2. General formulation

In interests of brevity, the notation of Craik & Criminale (1986) and Craik (1989) is followed and frequent reference is made to these papers, henceforth designated 'I' and 'II'. Although the present account should be comprehensible without constantly consulting these papers, derivations of results given in them are not repeated here.

Solutions of the incompressible Navier–Stokes equations, and hence of the inviscid Euler equations, are sought. As in I and II, these comprise a 'basic flow' of general form

$$U_i(x_j,t) = \sigma_{ij}(t)\,x_j + U_i^0(t) \quad (i,j = 1,2,3) \tag{2.1}$$

and a 'disturbance' in the form of a single Fourier mode

$$\begin{pmatrix} u_i' \\ p' \end{pmatrix} = \mathrm{Re}\left\{\begin{pmatrix} \hat{u}_i(t) \\ \hat{p}(t) \end{pmatrix} \exp\left[\mathrm{i}\alpha_j(t)\,x_j + \mathrm{i}\delta(t)\right]\right\}. \tag{2.2}$$

The governing equations for the velocity components of this single-mode disturbance turn out to be linear, without approximation. Likewise, linear superposition of modes with wavenumber vectors of identical orientation but differing magnitudes still yields exact solutions; but modes with differently directed wavenumber vectors interact nonlinearly. Here, we restrict attention to individual modes, with velocity components denoted by u_i' and associated pressures by p'. The admissible basic flows are linearly dependent on the space coordinates x_i and the flow domain is regarded as infinite. Attention will focus on time-periodic basic flows and, unlike II, the body force is taken to be zero. The elements σ_{ij} define a time-dependent matrix $\boldsymbol{S}(t)$ that must satisfy (see I, equation (2.4) or II, equation (2.6))

$$\mathrm{d}\boldsymbol{S}/\mathrm{d}t + \boldsymbol{S}^2 = \boldsymbol{M}(t)\ \text{(symmetric)}; \quad \mathrm{tr}\,(\boldsymbol{S}) = 0, \tag{2.3}$$

where $\boldsymbol{M}(t)$ is an arbitrary symmetric matrix.

For convenience, we restrict attention to basic flows with rates of strain that have principal directions, but not magnitudes, that are invariant in time and coincide with the coordinate axes. (This restriction may be relaxed.) We also set U_i^0 to zero. Accordingly,

$$\boldsymbol{S} = \{\sigma_{ij}(t)\} = \begin{pmatrix} a(t) & -\omega_3(t) & \omega_2(t) \\ \omega_3(t) & b(t) & -\omega_1(t) \\ -\omega_2(t) & \omega_1(t) & -a(t)-b(t) \end{pmatrix}, \tag{2.4}$$

where the three vorticity components $2w_j$ must satisfy (II, equation (4.3))

$$\omega_j(t) = \omega_{j0} \exp\left[\int_0^t \sigma_{jj}(t')\,\mathrm{d}t'\right]. \tag{2.5}$$

In this paper, we concentrate on sinusoidal strain rates

$$a(t) = a_0 \cos \Omega t, \quad b(t) = b_0 \cos \Omega t, \quad \Omega \text{ constant},$$

for which

$$\omega_1 = \omega_{10} \exp\left(\frac{a_0}{\Omega} \sin \Omega t\right), \quad \omega_2 = \omega_{20} \exp\left(\frac{b_0}{\Omega} \sin \Omega t\right), \quad \omega_3 = \omega_{30} \exp\left(-\frac{(a_0+b_0)}{\Omega} \sin \Omega t\right). \tag{2.6}$$

Additionally, we restrict attention to cases with $\omega_{10} = \omega_{20} = 0$: there is then only z-vorticity, stretched by the oscillatory strain rates. In contrast with the uniformly strained compressible flow examined in a linear approximation by Mansour & Lundgren (1990), our strained incompressible flows are necessarily three-dimensional and no approximations are involved except in §§3 and 5.

The variable wavenumber $\boldsymbol{\alpha}(t)$ of the disturbances satisfies (I, equation (2.6))

$$\mathrm{d}\alpha_j/\mathrm{d}t + \alpha_k \sigma_{kj} = 0, \quad \text{i.e. } \mathrm{d}\boldsymbol{\alpha}/\mathrm{d}t + \boldsymbol{S}^{\mathrm{T}}\boldsymbol{\alpha} = 0, \tag{2.7a}$$

which, for the basic flow (2.4), yields

$$\left.\begin{aligned} (\mathrm{d}/\mathrm{d}t + a_0 \cos \Omega t)\,\alpha_1 &= \omega_2 \alpha_3 - \omega_3 \alpha_2, \\ (\mathrm{d}/\mathrm{d}t + b_0 \cos \Omega t)\,\alpha_2 &= \omega_3 \alpha_1 - \omega_1 \alpha_3, \\ [\mathrm{d}/\mathrm{d}t - (a_0 + b_0) \cos \Omega t]\,\alpha_3 &= \omega_1 \alpha_2 - \omega_2 \alpha_1, \end{aligned}\right\} \tag{2.7b}$$

with the $\omega_j(t)$ as given in (2.6). It follows that

$$(\mathrm{d}/\mathrm{d}t)\,(\alpha_1 \omega_1 + \alpha_2 \omega_2 + \alpha_3 \omega_3) = 0,$$

which permits elimination of (say) α_3. Setting $\omega_{10} = \omega_{20} = 0$ and introducing new variables

$$\beta_1 \equiv \alpha_1 \hat{E}(a_0), \quad \beta_2 \equiv \alpha_2 \hat{E}(b_0), \tag{2.8a}$$

where

$$\hat{E}(\mu) \equiv \exp\left(\frac{\mu}{\Omega} \sin \Omega t\right),$$

gives

$$\left.\begin{aligned} \mathrm{d}\beta_1/\mathrm{d}t + \hat{E}(-2b_0)\,\omega_{30}\beta_2 &= \mathrm{d}\beta_2/\mathrm{d}t - \hat{E}(-2a_0)\,\omega_{30}\beta_1 = 0, \\ \alpha_3(t) &= \alpha_{30}\omega_{30}/\omega_3(t) = \alpha_{30}\hat{E}(a_0 + b_0). \end{aligned}\right\} \tag{2.8b}$$

Unfortunately, general closed-form solutions for β_1 and β_2 are unavailable. However, axisymmetric flows with $a_0 = b_0$ (which are studied in detail shortly) yield exact solutions.

The velocity components $u_j'(t)$ of the disturbance to the general flow (2.4) may be associated to those in the inviscid limit $\check{u}_j(t)$ by the substitution (I, equation (3.14))

$$\hat{u}_j(t) = \exp\left\{-\nu \int_0^t (\boldsymbol{\alpha}\cdot\boldsymbol{\alpha})\,\mathrm{d}t'\right\} \check{u}_i(t) \tag{2.9}$$

and the inviscid velocity components satisfy (I, (3.15))

$$\left.\begin{aligned} \mathrm{d}\check{\boldsymbol{u}}/\mathrm{d}t + \mathbb{T}\check{\boldsymbol{u}} &= \boldsymbol{0}, \quad \mathbb{T} = \{\tau_{ij}\}, \\ \tau_{ij} &= \sigma_{ij} - 2\alpha_i \alpha_k \sigma_{kj}/(\boldsymbol{\alpha}\cdot\boldsymbol{\alpha}), \end{aligned}\right\} \tag{2.10}$$

with the $\alpha_j(t)$ given in terms of their initial values α_{j0} by (2.8*b*). The associated pressure disturbance is also known (I, equation (2.9)) and, consistently with (2.10) and continuity,

$$\alpha_1 \check{u}_1 + \alpha_2 \check{u}_2 + \alpha_3 \check{u}_3 = 0, \tag{2.11}$$

which enables reduction of (2.10) to coupled equations for two variables.

For the present cases with $\omega_{10} = \omega_{20} = 0$, these can be written most compactly by introducing the new dependent variables

$$P \equiv \alpha_1 \check{u}_2 - \alpha_2 \check{u}_1, \quad Q \equiv |\boldsymbol{\alpha}(0)|\, \check{u}_3$$

and defining dimensionless quantities

$$\tau \equiv \Omega t, \quad \bar{a} \equiv \frac{a_0}{\Omega}, \quad \bar{b} \equiv \frac{b_0}{\Omega}, \quad \varpi \equiv \frac{2\omega_{30}\cos\theta_0}{\Omega}, \quad \theta_0 \equiv \tan^{-1}\left[\frac{(\alpha_{10}^2 + \alpha_{20}^2)^{\frac{1}{2}}}{\alpha_{30}}\right].$$

Then, after reduction, one finds

$$\mathrm{d}P/\mathrm{d}\tau = -(\bar{a}+\bar{b})P\cos\tau + \varpi Q, \tag{2.12a}$$

$$\frac{\mathrm{d}Q}{\mathrm{d}\tau} = \left\{-\frac{\varpi(\boldsymbol{\alpha}_0\cdot\boldsymbol{\alpha}_0)}{\boldsymbol{\alpha}\cdot\boldsymbol{\alpha}} - \frac{2(\bar{a}-\bar{b})\,|\boldsymbol{\alpha}_0|\,\alpha_1\alpha_2\alpha_3\cos\tau}{(\boldsymbol{\alpha}\cdot\boldsymbol{\alpha})(\alpha_1^2+\alpha_2^2)}\right\}P$$
$$+\left\{\frac{(\bar{a}+\bar{b})(\alpha_1^2+\alpha_2^2-2\alpha_3^2)}{\boldsymbol{\alpha}\cdot\boldsymbol{\alpha}} + \frac{(\bar{a}-\bar{b})(\alpha_2^2-\alpha_1^2)\alpha_3^2}{(\boldsymbol{\alpha}\cdot\boldsymbol{\alpha})(\alpha_1^2+\alpha_2^2)}\right\}Q\cos\tau \tag{2.12b}$$

together with (2.11).

Axisymmetric flows with $a_0 = b_0$

In axisymmetric cases with $a_0 = b_0$, (2.8) has solutions

$$\alpha_1 = \exp(-\bar{a}\sin\tau)B\cos\phi, \quad \alpha_2 = \exp(-\bar{a}\sin\tau)B\sin\phi,$$
$$\alpha_3 = \exp(2\bar{a}\sin\tau)\alpha_{30}, \tag{2.13}$$
$$B \equiv (\alpha_{10}^2+\alpha_{20}^2)^{\frac{1}{2}}, \quad \phi(\tau) \equiv \phi_0 + \frac{\omega_{30}}{\Omega}\int_0^\tau \exp(-2\bar{a}\sin\tau')\,\mathrm{d}\tau'.$$

It is convenient to re-express $\phi(\tau)$ as

$$\phi(\tau) = \phi_0 + (\omega_{30}/\Omega)I_0(-2\bar{a})\tau + \mathscr{F}(\tau), \tag{2.14}$$

where $I_0(\lambda)$ is the modified Bessel function

$$I_0(\lambda) \equiv \frac{1}{2\pi}\int_0^{2\pi}\exp(\lambda\sin\tau)\,\mathrm{d}\tau$$

and $\mathscr{F}(\tau)$ is the periodic function, with period 2π,

$$\mathscr{F}(\tau) \equiv \frac{\omega_{30}}{\Omega}\int_0^\tau\{\exp(-2\bar{a}\sin\tau') - I_0(-2\bar{a})\}\,\mathrm{d}\tau'.$$

It follows that the complex combination $\alpha_1 + \mathrm{i}\alpha_2$ is a product of periodic functions,

$$\alpha_1 + \mathrm{i}\alpha_2 = B\,\mathrm{e}^{\mathrm{i}\phi_0}\exp\left[\frac{\mathrm{i}\omega_{30}I_0(-2\bar{a})\tau}{\Omega}\right]\exp[-\bar{a}\sin\tau + \mathrm{i}\mathscr{F}(\tau)], \tag{2.15}$$

with respective periods 2π and $2\pi\Omega/\omega_{30}I_0(-2\bar{a})$.

On substituting these expressions for the α_j in (2.12), the velocity equations reduce to

$$\begin{pmatrix}\mathrm{d}P/\mathrm{d}\tau\\ \mathrm{d}Q/\mathrm{d}\tau\end{pmatrix} = \begin{pmatrix}-2\bar{a}\cos\tau & \varpi\\ \dfrac{-\varpi\sec^2\theta_0 E}{\tan^2\theta_0+E^3} & \dfrac{2\bar{a}\cos\tau(\tan^2\theta_0-2E^3)}{\tan^2\theta_0+E^3}\end{pmatrix}\begin{pmatrix}P\\ Q\end{pmatrix}. \tag{2.16}$$

Here $\bar{a}$, ϖ and θ_0 appear as parameters and

$$E(\tau) \equiv \exp(2\bar{a}\sin\tau).$$

Despite the two periodicities present in the wavenumber components α_1 and α_2, the 2×2 matrix of (2.16) is singly periodic, with period 2π. The second period disappears because of the axisymmetry of the basic flow; this means that α_1 and α_2 appear only in combination as their sum of squares. But the second period appears in the velocity equations if the strain rates a_0 and b_0 were unequal. Useful checks on the accuracy of (2.16) are that it agrees with the limiting cases, examined in I, of purely circular flow ($a_0 = 0$) and of steady axisymmetric stagnation-point flow ($\varpi = 0$ and $\Omega \to 0$).

An alternative formulation of (2.16) as a single second-order equation is

$$\frac{\mathrm{d}^2V}{\mathrm{d}\tau^2}+V\left\{\frac{\varpi^2\sec^2\theta_0E^{-2}}{1+T}+\bar{a}\sin\tau\left(\frac{1-2T}{1+T}\right)-\bar{a}^2\cos^2\tau\left(\frac{1+14T+4T^2}{(1+T)^2}\right)\right\}=0, \quad (2.17)$$

where $V(\tau)$ is defined as

$$V(\tau)\equiv P\exp\int_0^\tau\frac{3\bar{a}\cos\tau'}{1+T(\tau')}\mathrm{d}\tau'$$

and, for brevity, $T(\tau)\equiv\tan^2\theta_0E^{-3}(\tau)$. Since the coefficient of V is periodic in τ, this has the form of a Hill's equation (see Magnus & Winkler 1966).

As the governing equations are linear and time-periodic, the stability problem may be solved by direct application of Floquet theory, as in the case of elliptical instability.

3. Weakly oscillating axisymmetric flows

When the oscillatory stagnation-point flow is weak compared with the rotational motion, the parameter $\bar{a}$ is small and the above equations may be expressed, to good approximation, by truncated power series in $\bar{a}$. From (2.17), it is found after some effort that

$$\begin{aligned}\mathrm{d}^2V/\mathrm{d}\tau^2+V\{&\varpi^2+\bar{a}^2(9C^2-6C-4)+\bar{a}\sin\tau[\varpi^2(2-6C)+(3C-2)]\\&+\bar{a}^2\sin^2\tau[\varpi^2(36C^2-30C+2)+(-27C^2+24C+4)]+O(\bar{a}^3)\}=0,\end{aligned} \quad (3.1)$$

where $C\equiv\cos^2\theta_0$. If terms of $O(\bar{a}^2)$ are neglected, this reduces to Mathieu's equation,

$$\mathrm{d}^2V/\mathrm{d}\tau^2+V\{\varpi^2+\bar{a}\sin\tau[\varpi^2(2-6C)+(3C-2)\}=0, \quad (3.2)$$

the stability properties of which are well-known (see e.g. Kevorkian & Cole 1981). The first unstable region, centred on $\varpi^2=\frac{1}{4}$, has width

$$|\varpi^2-\tfrac{1}{4}|<|\tfrac{1}{2}\bar{a}[\varpi^2(2-6C)+(3C-2)]|\approx\tfrac{3}{4}|\bar{a}|\sin^2\theta_0 \quad (3.3)$$

for small $\bar{a}$. The second band of instability of Mathieu's equation is centred on $\varpi^2=1$. However, since the bandwidth of this unstable region is of $O(\bar{a}^2)$, Mathieu's equation is unable to determine whether instability exists near $\varpi^2=1$ for the original equation (2.17). For this, the terms of $O(\bar{a}^2)$ must be retained.

The first few regions of instability of the equation

$$\mathrm{d}^2y/\mathrm{d}t^2+(\lambda+\gamma_1\cos t+\gamma_2\cos 2t)\,y=0$$

have been determined numerically by Klotter & Kotowski (1943), the three-dimensional parameter surfaces being ingeniously displayed by photographs of cardboard models. Our equation (3.1) is obviously of this form. Also, Magnus & Winkler (1966) comprehensively describe the theory of Hill's equation. However, only the limiting case of small $\bar{a}$ is relevant here: perturbation techniques described by Kevorkian & Cole (1981) and Nayfeh & Mook (1979) then suffice to determine the first and second stability boundaries.

The first instability region, if attainable, is characterized by the largest growth rates and so is less likely to be suppressed by viscous decay (see (2.9)). The value $\varpi^2=\frac{1}{4}$ corresponds to

$$\omega_{30}\cos\theta_0=\pm\tfrac{1}{4}\Omega$$

in the original variables, and the width of the region of inviscid instability centred upon it is given in (3.3). This instability region is attainable only if $|\omega_{30}/\Omega|>\frac{1}{4}$ and

the most unstable wavenumbers are initially inclined at an angle $\cos^{-1}|\Omega/4\omega_{30}|$ to the axis of symmetry of the basic flow. The second region of instability, centred on $\varpi^2 = 1$, is attainable only if $|\omega_{30}/\Omega| > \frac{1}{2}$. The latter condition is more stringent than the former and the second region of instability is narrower, of $O(\bar{a}^2)$. Consequently, for $\bar{a}$ small, the dominant instability is certainly that with $\varpi^2 \approx \frac{1}{4}$.

4. Numerical results and discussion

In order to solve equation (2.16) a fourth-order Runge–Kutta–Merson scheme was employed on a Sunsparc 1+ Workstation running at 12.5 MIPS. The scheme was known to be highly reliable from previous experience of other problems. It employed an adaptive step-size control to achieve a predetermined local truncation error or tolerance. All calculations were done in double precision and the local truncation error was set initially to 10^{-6}. When necessary, this was refined to 10^{-10}. Occasional checks on the global error were made by reducing the tolerance to 10^{-9} and discovering how many significant figures were unaffected by this change. It was concluded that a tolerance of 10^{-6} was often adequate, but that the greater accuracy was needed in order to distinguish some very narrow regions of instability (see below).

The procedure employed was that suggested by Floquet theory and is similar to (but numerically much more accurate than) that of II. With chosen values of ω_{30}/Ω, $\bar{a}$ and θ_0, (2.16) was first solved with starting values $(P, Q) = (1, 0)$ at $\tau = 0$ to find (P_1, Q_1) at $\tau = 2\pi$. Then with starting values $(0, 1)$, (P_2, Q_2) at $\tau = 2\pi$ were similarly calculated. It is known from theory that the resulting matrix

$$\boldsymbol{N} = \begin{pmatrix} P_1 & P_2 \\ Q_1 & Q_2 \end{pmatrix}$$

must have its determinant equal to unity; and this was so to high accuracy in the computations. The eigenvalues of $\boldsymbol{N}$ are

$$\lambda_1, \lambda_2 = \tfrac{1}{2}\operatorname{tr}\boldsymbol{N} \pm [\tfrac{1}{4}(\operatorname{tr}\boldsymbol{N})^2 - 1]^{\frac{1}{2}}, \tag{4.1}$$

and Floquet theory (see II, p. 281) shows that any disturbance (P, Q) is a linear combination of two modes

$$e^{\sigma_1 \tau}(p_1, q_1), \quad e^{\sigma_2 \tau}(p_2, q_2),$$

where the $p_i(t)$ and $q_i(t)$ are periodic functions with period 2π and the σ_i are related to the eigenvalues of $\boldsymbol{N}$ by

$$\sigma_i = \frac{1}{2\pi}\log \lambda_i. \tag{4.2}$$

There is instability whenever $\operatorname{Re}\{\sigma_i\} > 0$: that is, whenever the trace, $\operatorname{tr}(\boldsymbol{N})$, of $\boldsymbol{N}$ exceeds 2 or is less than -2. The stability boundaries with $\operatorname{tr}(\boldsymbol{N}) = 2$ correspond to solutions with period 2π and those with $\operatorname{tr}(\boldsymbol{N}) = -2$ correspond to solutions with period π. As is normal for equations of Hill type (see Magnus & Winkler 1966), these yield two interleaved families of instability bands.

The computations yielded values of $\operatorname{tr}(\boldsymbol{N})$ for θ_0 in the range $[0, \frac{1}{2}\pi]$ at chosen values of $\bar{a}$ and ω_{30}/Ω. The case $\omega_{30}/\Omega = 2$ was investigated in great detail, for $\bar{a}$ in the range $[0, 2]$ with increments of 0.1. Other values of ω_{30}/Ω were also investigated: enough results, both theoretical and computational, are described below to indicate the general character of the solutions. Accordingly, we have resisted the temptation to present many additional graphs of results at various ω_{30}/Ω.

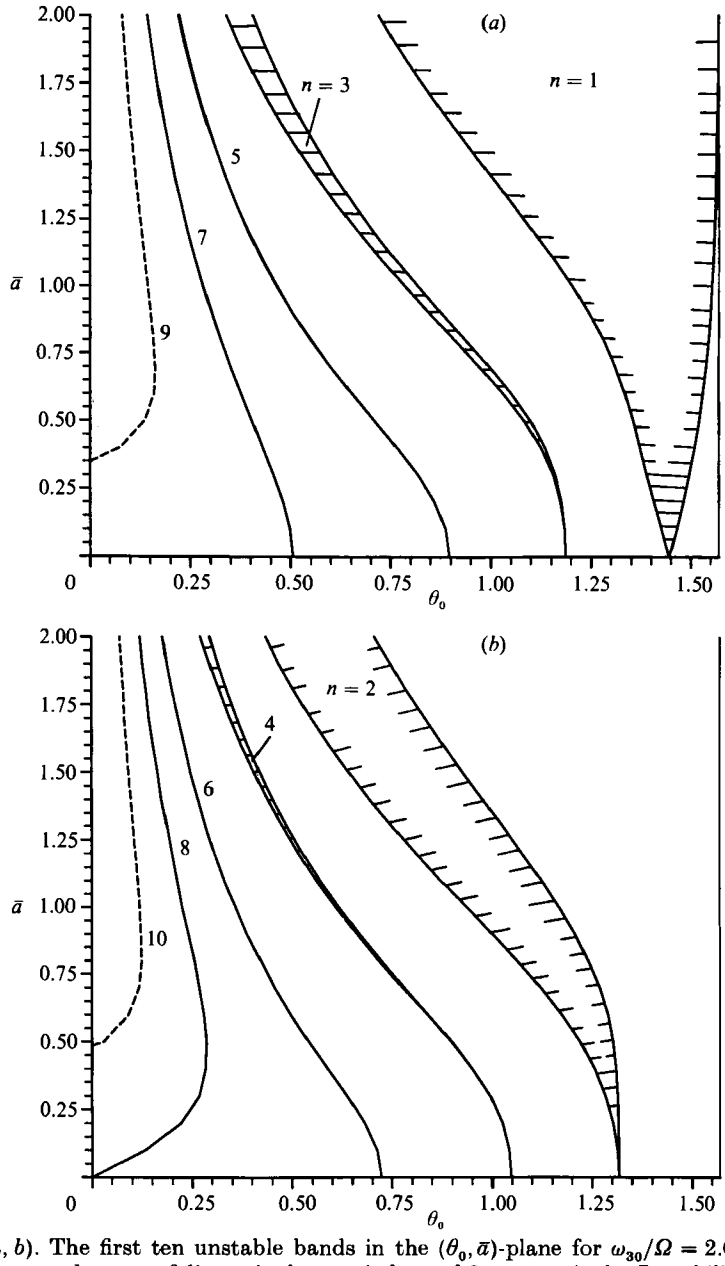

FIGURE 1 (*a*, *b*). The first ten unstable bands in the $(\theta_0, \bar{a})$-plane for $\omega_{30}/\Omega = 2.0$. Odd and even modes have neutral states of dimensionless period π and 2π respectively. Instability bands become progressively narrower as the mode number n increases: those with $n = 9$ and 10 are at the limit of accuracy of our computations.

Results for $\omega_{30}/\Omega = 2$ are shown in figures 1 (*a*) and 1 (*b*), where the horizontal axis is θ_0 and the vertical is $\bar{a} = a_0/\Omega$. The plotted curves show regions of instability; those in figure 1 (*a*) are for modes with $\mathrm{tr}\,(\boldsymbol{N}) < -2$ and those in figure 1 (*b*) are for modes with $\mathrm{tr}\,(\boldsymbol{N}) > 2$. Only two of these regions, labelled $n = 1$ and 2, are extensive, as indicated by cross-hatching. Regions $n = 3$ and 4 are much narrower though visible on the scale of the figures, while the others with $n > 4$ are usually narrower than the thickness of the lines shown.

Mode n	1	2	3	4	5	6	7	8
θ_0	1.4435	1.0677	0.8015	0.6125	0.4644	0.3576	0.2809	0.2248
tr $(\boldsymbol{N})$	−38.68	6.463	−2.066	2.0056	−2.000027	2.000023*	−2.000006*	2.000003*
Re$\{\sigma\}$	0.582	0.293	0.041	0.012	0.00083	0.00077*	0.00038*	0.00027*

TABLE 1. Maximum values of tr $(\boldsymbol{N})$ and growth rate Re$\{\sigma\}$ of the first eight modes, with corresponding angles θ_0, for $\omega_{30}/\Omega = 2$ and $\bar{a} = 1$. The accuracy of results marked with an asterisk is not guaranteed.

Results for small $\bar{a}$ agree with expectations for equations of Hill type, with regions of parametric instability emanating from

$$\varpi^2 = \left(\frac{2\omega_{30}\cos\theta_0}{\Omega}\right)^2 = \tfrac{1}{4}n^2 \quad (n = 1, 2, 3, 4\ldots). \tag{4.3}$$

With $\omega_{30}/\Omega = 2$, this yields eight roots, namely $\theta_0 = 1.3181$, 1.0472, 0.7227 and 0 radians for $n = 2, 4, 6, 8$, and $\theta_0 = 1.4455$, 1.1864, 0.8957, 0.5054 radians for $n = 1, 3, 5, 7$ respectively. This is precisely as found numerically. Notice, too, that the number of instability bands emanating from the axis $\bar{a} = 0$ increases as ω_{30}/Ω increases. For $0 < \omega_{30}/\Omega < \frac{1}{4}$ there are none, for $\frac{1}{4} < \omega_{30}/\Omega < \frac{1}{2}$ there is just one and for $\omega_{30}/\Omega = 1$ there are four. The number of such bands equals the largest integer less than or equal to $4\omega_{30}/\Omega$.

The first region of instability is much the strongest, as expected; for it is known that, at small $\bar{a}$, the respective growth rates are of $O(\bar{a}^n)$ and these are confined to bandwidths of similar orders of magnitude. This means that it is very hard to detect the higher-order instabilities when $\bar{a}$ is small. Accordingly, a slight compromise proved necessary in plotting figure 1: for $n > 4$ the points plotted are those for which tr $(\boldsymbol{N})$ exceeds 1.999 rather than 2: however, it should be emphasized that clear evidence of instability, with tr $(\boldsymbol{N}) > 2$, was found at some values of $\bar{a}$ for all the n-values shown.

To give a clearer impression of just how weak the higher-order instabilities are, we show in table 1 above the greatest value of tr $(\boldsymbol{N})$ found at $\bar{a} = 1$ and $\omega_{30}/\Omega = 2$ for the first eight instability regions. To detect the last two, a very fine mesh for θ_0 was needed. Also shown are the values of θ_0 and the maximum growth rate Re$\{\sigma\}$ calculated from (4.1) and (4.2). Of course, as was mentioned earlier, weakly growing instabilities will be susceptible to suppression by viscosity through the additional decay factor present in (2.9). The instability bands are exceedingly narrow for the larger n-values: for example, those with $n = 6$ and $n = 8$ are $0.35744 < \theta_0 < 0.35774$ and $0.22476 < \theta_0 < 0.22481$ respectively.

In contrast, the lowest modes can have remarkably large growth rates. The dimensional e-folding time is $[2\pi\,\mathrm{Re}\{\sigma\}]^{-1}$ times the oscillation period $2\pi/\Omega$. For the $n = 1$ mode of table 1, this is less than one third of the period of oscillation and so only a few periods would normally be required for this mode to grow to prominence.

There was much numerical evidence that, when $\bar{a}$ is large, more instability bands are present than originate from the axis $\bar{a} = 0$. Only two of these, labelled $n = 9$ and 10, are shown in figure 1 (a, b): the other bands are too thin and the instabilities too weak for our results to be relied on and are therefore omitted. The various bands of instability may be roughly explained as follows. Equation (2.17) has the form

$$\mathrm{d}^2V/\mathrm{d}\tau^2 + R(\tau)\,V = 0, \quad R(\tau) = R(\tau + 2\pi)$$

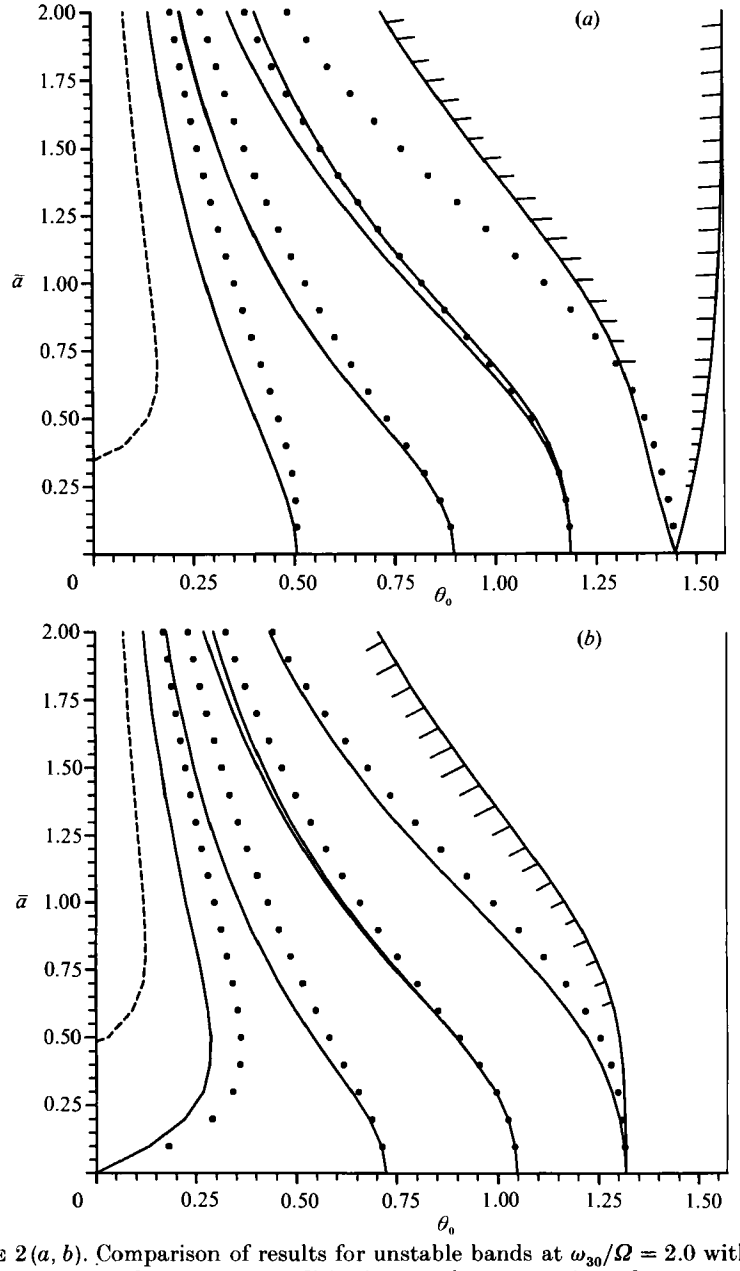

FIGURE 2(*a*, *b*). Comparison of results for unstable bands at $\omega_{30}/\Omega = 2.0$ with the intuitive 'averaged resonance condition' (4.4) (shown as points) for $n = 1$ to 8.

and one might expect parametric-resonance instabilities to be centred on the 'average frequencies' satisfying

$$\frac{1}{2\pi}\int_0^{2\pi} R(\tau)\,\mathrm{d}\tau = \tfrac{1}{4}n^2 \quad (n = 1, 2, 3, \ldots). \tag{4.4}$$

Though plausible, this criterion has no precise theoretical foundation except when $\bar{a}$ is small: accordingly, we carried out a comparison of (4.4) with the exact results shown in figure 1 (*a*, *b*). Equation (4.4) was solved iteratively for θ_0 with the first eight

n	Unstable bandwidth	Max tr($\boldsymbol{N}$)	θ_0	Re{σ}
1	$0.01625 < \theta_0 < 0.2848$	-8.25586	0.04057	0.3336
2	$9.42\times10^{-3} < \theta_0 < 1.005\times10^{-2}$	2.02017	9.731×10^{-3}	2.26×10^{-2}
3	$4.711\times10^{-3} < \theta_0 < 4.784\times10^{-3}$	-2.00111	4.747×10^{-3}	5.31×10^{-3}
4	$1.966\times10^{-3} < \theta_0 < 1.974\times10^{-3}$	2.000026	1.970×10^{-3}	8.193×10^{-4}

TABLE 2. Results for $\omega_{30}/\Omega = 0.1$, $\bar{a} = 2.0$. Four unstable bands were found as shown. The maxima of $|\mathrm{tr}(\boldsymbol{N})|$, the corresponding θ_0 and maximum growth rate Re{σ} are also shown. Note that all except the $n = 1$ instability band are confined to very small θ_0 values.

values $n = 1, 2, \ldots, 8$ at various values of $\bar{a}$ and with $\varpi_{30}/\Omega = 2$. The results are shown as points in figure 2(a, b), where they may be compared with the precise regions of instability repeated from figure 1(a, b). Agreement is good at small values of $\bar{a}$, but this deteriorates as $\bar{a}$ increases.

Nevertheless, this rough qualitative agreement is enough to provide an explanation of the emergence of new instability bands from the $\theta_0 = 0$ axis as $\bar{a}$ increases. The criterion (4.4) reduces to

$$4\omega_{30}^2 I_0(4\bar{a})/\Omega^2 = \tfrac{1}{2}\bar{a}^2 + \tfrac{1}{4}n^2 \tag{4.5}$$

when $\theta_0 = 0$. With $\omega_{30}/\Omega = 2$, this has roots with $(n, \bar{a})$ equal to (8, 0), (9, 0.25), (10, 0.35), (11, 0.43), (12, 0.50) approximately, the values of the Bessel function $I_0(x)$ being taken from the tables of Abramowitz & Stegun (1965). In fact, these roots yield considerable underestimates of the true unstable values of $\bar{a}$ obtained directly from the full equation (2.16). For example, the values of $\bar{a}$ shown on the axis $\theta_0 = 0$ in figure 1(a, b) for $n = 8$, 9 and 10 are 0, 0.35 and 0.48 respectively. Despite the inaccuracy of the 'frequency-averaged' criterion (4.4), its roots correctly identify the general character of the instabilities as associated with higher-order parametric resonance.

We also examined in detail the case $\omega_{30}/\Omega = 0.1$ and $\bar{a} = 2$. At this low value of ω_{30}/Ω, there is no instability at any value of θ_0 when $\bar{a}$ is small; but at $\bar{a} = 2$, we found the four unstable bands and maximum growth rates shown in table 2.

On recalling that $\bar{a} = a_0/\Omega$, our results indicate that: (i) *at any given frequency* Ω, *all flows with non-zero rotation rates* ω_{30} *are destabilized by sufficiently large oscillatory rates of strain* a_0 (even though instability at small rates of strain is restricted to $\omega_{30} > \frac{1}{4}\Omega$); (ii) *with any given* $a_0 > 0$, *all flows with non-zero rotation rates* ω_{30} *are destabilized when the forcing frequency* Ω *is sufficiently small*; (iii) *when* a_0/Ω *is* 0(1), *inviscid growth rates of the lowest modes can be sufficiently large for waves to appear within a few oscillation periods.*

5. Non-axisymmetric flows with small-amplitude forcing

Non-axisymmetric 'basic' flows with $a_0 \neq b_0$ are governed by (2.8), (2.11) and (2.12). In principle, for given initial data, (2.8) may be solved to find $\boldsymbol{\alpha}(t)$ and substitution in (2.12) still yields a linear problem for P and Q. But now the coefficients of P and Q in (2.12) need not be singly periodic in τ and so Floquet theory is not applicable. Nevertheless, direct computation would still yield the evolutionary behaviour of particular cases. Instead, we here develop the approximate theory, valid for small a_0 and b_0, that is equivalent to – but more complicated than – that for axisymmetric flows given in §3.

With a_0 and b_0 small, of order ϵ say, the basic solid-body rotation about the z-axis

is only slightly altered by small non-axisymmetric time-periodic fluctuations. The following theory describes the evolution of single-mode disturbances up to arbitrarily large amplitudes, in response to such small-amplitude forcing.

Equations (2.8*b*) then simplify to

$$\left.\begin{aligned} \mathrm{d}\beta_1/\mathrm{d}t+\omega_{30}\beta_2 &= \epsilon\tilde{b}\sin(\Omega t)\,\beta_2+O(\epsilon^2),\\ \mathrm{d}\beta_2/\mathrm{d}t-\omega_{30}\beta_1 &= -\epsilon\tilde{a}\sin(\Omega t)\,\beta_1+O(\epsilon^2),\\ \text{where}\qquad 2\omega_{30}a_0/\Omega &\equiv \epsilon\tilde{a},\quad 2\omega_{30}b_0/\Omega\equiv\epsilon\tilde{b} \end{aligned}\right\} \tag{5.1}$$

and $\tilde{a}$, $\tilde{b}$ are $O(1)$ constants.

Series expansion of β_1 and β_2 as

$$\beta_j=\beta_j^{(0)}+\epsilon\beta_j^{(1)}+\ldots$$

$$\left.\begin{aligned} &\text{leads to}\qquad \beta_1^{(0)}=B_0\cos(\omega_{30}t+\phi_0),\quad \beta_2^{(0)}=B_0\sin(\omega_{30}t+\phi_0),\\ &\left.\begin{aligned} \mathrm{d}\beta_1^{(1)}/\mathrm{d}t+\omega_{30}\beta_2^{(1)} &= \tilde{b}B_0\sin(\Omega t)\sin(\omega_{30}t+\phi_0)\\ \mathrm{d}\beta_2^{(1)}/\mathrm{d}t-\omega_{30}\beta_1^{(1)} &= -\tilde{a}B_0\sin(\Omega t)\cos(\omega_{30}t+\phi_0) \end{aligned}\right\}(B_0,\phi_0\ \text{constant}). \end{aligned}\right\} \tag{5.2}$$

The latter equations have the general solution

$$\left.\begin{aligned} \beta_1^{(1)} &= B_1\cos(\omega_{30}t+\phi_1)+\tfrac{1}{4}B_0\sin[(\Omega+\omega_{30})t+\phi_0]\left\{\frac{-(\tilde{a}+\tilde{b})}{\Omega}+\left(\frac{\tilde{a}-\tilde{b}}{\Omega+2\omega_{30}}\right)\right\}\\ &\quad+\tfrac{1}{4}B_0\sin[(\omega_{30}-\Omega)t+\phi_0]\left\{-\frac{(\tilde{a}+\tilde{b})}{\Omega}+\left(\frac{\tilde{a}-\tilde{b}}{\Omega-2\omega_{30}}\right)\right\},\\ \beta_2^{(1)} &= B_1\sin(\omega_{30}t+\phi_1)+\tfrac{1}{4}B_0\cos[(\Omega+\omega_{30})t+\phi_0]\left\{\frac{(\tilde{a}+\tilde{b})}{\Omega}+\left(\frac{\tilde{a}-\tilde{b}}{\Omega+2\omega_{30}}\right)\right\}\\ &\quad+\tfrac{1}{4}B_0\cos[(\omega_{30}-\Omega)t+\phi_0]\left\{\frac{(\tilde{a}+\tilde{b})}{\Omega}+\left(\frac{\tilde{a}-\tilde{b}}{\Omega-2\omega_{30}}\right)\right\}, \end{aligned}\right\} \tag{5.3}$$

and B_1 may be set to zero without loss. The corresponding wavenumber components are then easily found from (2.8*a*) with $O(\epsilon^2)$ error.

Substitution in (2.12) and retention of only leading terms in ϵ is straightforward but tedious. With $\theta_0\equiv\tan^{-1}(B_0/\alpha_{30})$ and reversion to the notation introduced above (2.12), equation (2.12*b*) yields

$$\begin{aligned} \frac{\mathrm{d}Q}{\mathrm{d}\tau} &= Q\cos\tau\{(\bar{a}+\bar{b})(\sin^2\theta_0-2\cos^2\theta_0)-(\bar{a}-\bar{b})\,2\cos^2\theta_0\cos[(2\omega_{30}/\Omega)\tau+2\phi_0]\}\\ &\quad+P\{-\varpi+2\varpi(\bar{a}+\bar{b})\cos^2\theta_0\sin\tau-(\bar{a}-\bar{b})\cos\theta_0\cos\tau\sin[(2\omega_{30}/\Omega)\tau+2\phi_0]\\ &\quad-2\varpi\sin\tau\left[\frac{\bar{a}B_0^2\cos^2\langle(\omega_{30}/\Omega)\tau+\phi_0\rangle+\bar{b}B_0^2\sin^2\langle(\omega_{30}/\Omega)\tau+\phi_0\rangle}{B_0^2+\alpha_{30}^2}\right]+\mathscr{G}\Big\} \end{aligned} \tag{5.4}$$

at this order. Here,

$$\begin{aligned} \mathscr{G} &\equiv \left(\frac{-\epsilon B_0}{B_0^2+\alpha_{30}^2}\right)[\beta_1^{(1)}\cos\langle(\omega_{30}/\Omega)\tau+\phi_0\rangle+\beta_2^{(1)}\sin\langle(\omega_{30}/\Omega)\tau+\phi_0\rangle]\\ &= \left(\frac{-(\bar{a}-\bar{b})B_0^2\omega_{30}}{B_0^2+\alpha_{30}^2}\right)\left\{\frac{\sin(\sigma^+\tau+2\phi_0)}{\Omega+2\omega_{30}}+\frac{\sin(\sigma^-\tau+2\phi_0)}{\Omega-2\omega_{30}}\right\}, \end{aligned}$$

$$\sigma^{\pm}\equiv\varpi\sec\theta_0\pm1=\frac{2\omega_{30}}{\Omega}\pm1.$$

Further reduction eventually leads to

$$\frac{\mathrm{d}}{\mathrm{d}\tau}\begin{pmatrix}P\\Q\end{pmatrix} = \mathbb{M}(\tau)\begin{pmatrix}P\\Q\end{pmatrix}, \tag{5.5}$$

$$\mathbb{M} \equiv \begin{pmatrix} -(\bar{a}+\bar{b})\cos\tau & \varpi \\ [-\varpi+\varpi f\sin\tau+g^+\sin(\sigma^+\tau+2\phi_0) & [-f\cos\tau+h\cos(\sigma^+\tau+2\phi_0) \\ \quad +g^-\sin(\sigma^-\tau+2\phi_0)] & \quad +h\cos(\sigma^-\tau+2\phi_0)] \end{pmatrix},$$

$$f \equiv (\bar{a}+\bar{b})(3\cos^2\theta_0-1), \quad g^\pm \equiv \mp(\bar{a}-\bar{b})R(\varpi, \pm\cos\theta_0), \quad h \equiv -(\bar{a}-\bar{b})\cos^2\theta_0,$$

$$R(\varpi, c) \equiv [c^2+\varpi(1+2c-c^2-c^3)+\varpi^2(1-c^2)]/(c+\varpi),$$

where each coefficient of the matrix $\mathbb{M}$ is correct at $O(\epsilon)$.

The system (5.5) may be recast as a single second-order equation by eliminating Q. Its first time-derivative is then removed by introducing

$$\mathscr{V} \equiv P\exp\left\{\tfrac{1}{2}\cos^2\theta_0\left\langle 3(\bar{a}+\bar{b})\sin\tau+(\bar{a}-\bar{b})\left[\frac{\sin(\sigma^+\tau+2\phi_0)}{\sigma^+}+\frac{\sin(\sigma^-\tau+2\phi_0}{\sigma^-}\right]\right\rangle\right\},$$

which satisfies

$$\frac{\mathrm{d}^2\mathscr{V}}{\mathrm{d}\tau^2} = -\mathscr{V}\{\varpi^2+(\bar{a}+\bar{b})\hat{T}\sin\tau+(\bar{a}-\bar{b})[S^+\sin(\sigma^+\tau+2\phi_0)+S^-\sin(\sigma^-\tau+2\phi_0)]\}, \tag{5.6}$$

where

$$\hat{T} \equiv 3\cos^2\theta_0(\tfrac{1}{2}-\varpi^2)+(\varpi^2-1), \quad S^\pm \equiv \tfrac{1}{2}(\varpi\pm\cos\theta_0)\cos\theta_0 \pm \varpi R(\varpi, \pm\cos\theta_0).$$

When $\bar{a}=\bar{b}$, this reduces to the Mathieu equation (3.2); but, with $\bar{a}\neq\bar{b}$, it has three separate forcing terms with differing frequencies. This equation is of Hill type only when σ^+ and σ^- are rational numbers and usefully so only when these numbers are ratios of quite small integers. Despite recent progress, the basic theory is incomplete for frequencies that are not rationally related: accordingly, the stability properties of (5.6) are not fully understood.

However, when the forcing parameters $\bar{a}$ and $\bar{b}$ are small, as here, a method described by Kevorkian & Cole (1981) may be applied to determine the dominant instability bands. In short, each forcing term is responsible for a region of instability centred on half its own frequency; namely

$$|\varpi^2-\tfrac{1}{4}| < \tfrac{1}{2}|(\bar{a}+\bar{b})\hat{T}| \approx \tfrac{3}{8}|\bar{a}+\bar{b}|\sin^2\theta_0, \tag{5.7a}$$

$$|\varpi^2-\tfrac{1}{4}(\sigma^+)^2| < \tfrac{1}{2}(\sigma^+)^{-2}|(\bar{a}-\bar{b})S^+|, \tag{5.7b}$$

$$|\varpi^2-\tfrac{1}{4}(\sigma^-)^2| < \tfrac{1}{2}(\sigma^-)^{-2}|(\bar{a}-\bar{b})S^-|. \tag{5.7c}$$

Weaker, less important regions of instability also occur at higher order in ϵ, centred on higher harmonics and sum-and-difference frequencies.

In terms of original variables, the above three unstable frequency bands are centred on

$$\frac{\omega_{30}}{\Omega} = \frac{1}{\pm 4\cos\theta_0}, \quad \frac{-1}{2\pm 4\cos\theta_0}, \quad \frac{1}{2\pm 4\cos\theta_0}. \tag{5.8a–c}$$

Since $-1 < \cos\theta_0 < 1$, these are respectively attainable for some wavenumber orientation provided ω_{30}/Ω lies outside the intervals $(-\frac{1}{4}, \frac{1}{4})$, $(-\frac{1}{6}, \frac{1}{2})$, $(-\frac{1}{2}, \frac{1}{6})$. Clearly, when $|\omega_{30}/\Omega| < \frac{1}{6}$, *none* of these resonances can happen: that is to say, the three potentially most important parametric instabilities arise for weak forcing only if the

frequency Ω is sufficiently small relative to the basic vorticity $2\omega_{30}$. When $|\omega_{30}/\Omega|$ is large, the non-axisymmetric resonances (5.8*b*, *c*) approach $\cos\theta_0 = \pm\frac{1}{2}$: as expected, these are the values of θ_0 for instability of steady elliptical flows (Bayly 1986).

Fuller examination of the unstable parameter ranges of (5.5) and the more general (2.12) must be postponed. For related problems in structural mechanics, Barr & McWhannell (1971) and Othman, Watt & Barr (1987) report interesting numerical results on low-frequency instabilities excited by three separate higher, but rationally related, frequencies. For incommensurate frequencies, some fundamental issues are addressed by Johnson & Moser (1982).

6. Conclusions

Three-dimensional uniformly rotating flows subjected to time-periodic, spatially uniform strain rates support parametric-type instabilities of plane-wave disturbances. The inviscid theory is exact for all disturbance amplitudes and extension to include viscosity in straightforward.

For strain rates that are symmetric about the axis of rotation, plane waves are governed by equations of Hill type; and, when these strain rates are sufficiently small, the primary region of instability is determined by a Mathieu equation. For larger periodic strain rates, Floquet theory allied to numerical computation determined various bands of instability, as fully described in §4. Growth rates of the main instability bands can be large, with e-folding times of the same order as, or even smaller than, the oscillation period $2\pi/\Omega$; but higher-order instability bands have much smaller growth rates.

With non-axisymmetric strain rates, the situation is more complex, for several forcing frequencies then coexist within the governing equations. Results at small forcing amplitudes are described in §5, where it is shown that the axisymmetric parametric instability is joined by others related to the previously known instability of elliptical flows.

Despite the idealizations inherent in our exact solutions, the results have relevance to the breakdown or persistence of eddies within turbulence, for the centre of such an eddy is certainly described locally by our analysis. We have shown that internal instabilities of parametric-resonance type occur, centred on specific wavenumber bands and certain ranges of frequency. But imposed frequencies that are too large compared with the eddy's vorticity cannot cause such instability, at least with small-amplitude forcing.

Of course, for finite eddies, additional modes of instability can arise by distortion of the boundaries (here taken to be at infinity) or on account of a non-uniform vorticity distribution: cf. Dritschel (1986, 1990). Also, the plane-wave structure imposed here is incompatible with boundary conditions at fixed walls. Nevertheless, as mentioned in the introduction, previous studies of elliptical instability show an encouraging connection between the growth rates of unstable normal modes in finite domains and those of unbounded plane waves. The same is likely to be so for the parametric instabilities discussed here.

This work was initiated during a visit by A.D.D.C. to the University of Washington in summer 1990, funded by the USAF Window on Science Program. Useful discussions with W. O. Criminale and B. Long, the hospitality of the Department of Applied Mathematics and the support of USAF are gratefully acknowledged. So, too, are comments by Professor W. Craig and the referees.

REFERENCES

ABRAMOWITZ, M. & STEGUN, I. A. (eds.) 1965 *Handbook of Mathematical Functions*. Dover.

BARR, A. D. S. & MCWHANNELL, D. C. 1971 *J. Sound Vib.* **14**, 491–509.

BAYLY, B. J. 1986 *Phys. Rev. Lett.* **57**, 2160–2171.

BAYLY, B. J., ORSZAG, S. A. & HERBERT, T. 1989 *Ann. Rev. Fluid Mech.* **20**, 359–391.

BENJAMIN, T. B. & URSELL, F. 1954 *Proc. R. Soc. Lond.* A **225**, 505–515.

CRAIK, A. D. D. 1985 *Wave Interactions and Fluid Flows*. Cambridge University Press.

CRAIK, A. D. D. 1988 *Proc. R. Soc. Lond.* A **417**, 235–244.

CRAIK, A. D. D. 1989 *J. Fluid Mech.* **198**, 275–292 (referred to herein as II).

CRAIK, A. D. D. 1991 In *Nonlinear Dynamics of Structures : Proc. Internat. Symp. Perm-Moscow* (ed. R. Z. Sagdeev, U. Frisch, S. S. Moiseev & N. Erokhin), pp. 289–293. World Scientific.

CRAIK, A. D. D. & CRIMINALE, W. O. 1986 *Proc. R. Soc. Lond.* A **406**, 13–26 (referred to herein as I).

DRITSCHEL, D. G. 1986 *J. Fluid Mech.* **172**, 157–182.

DRITSCHEL, D. G. 1990 *J. Fluid Mech.* **210**, 223–261.

FARADAY, M. 1831 *Phil. Trans. R. Soc. Lond.* **121**, 299–340.

GLEDZER, E. B., DOLZHANSKY, F. V., OBUKHOV, A. M. & PONOMAREV, V. M. 1975 *Izv. Atmos. Ocean. Phys.* **11**, 617–622.

GLEDZER, E. B. & PONOMAREV, V. M. 1992 Elliptical instability theory of bounded flows. *J. Fluid Mech.* (submitted).

HAYNES, P. H. 1987 *J. Fluid Mech.* **175**, 463–478.

JOHNSON, R. & MOSER, J. 1982 *Commun. Math. Phys.* **84**, 403–438.

KELVIN, LORD 1887 *Phil. Mag.* **24** (5), 188–196.

KEVORKIAN, J. & COLE, J. D. 1981 *Perturbation Methods in Applied Mathematics*. Springer.

KLOTTER, K. & KOTOWSKI, G. 1943 *Z. Angew. Math. Mech.* **23**, 149–155.

LAGNADO, R. R., PHAN-THIEN, N. & LEAL, L. G. 1984 *Phys. Fluids* **27**, 1094–1101.

LANDMAN, M. J. & SAFFMAN, P. G. 1987 *Phys. Fluids* **30**, 2339–2342.

MCEWAN, A. D. & ROBINSON, R. M. 1975 *J. Fluid Mech.* **67**, 667–687.

MAGNUS, W. & WINKLER, S. 1966 *Hill's Equation*. Wiley.

MALKUS, W. V. R. 1989 *Geophys. Astrophys. Fluid Dyn.* **48**, 123–143.

MANSOUR, N. N. & LUNDGREN, T. S. 1990 *Phys. Fluids* A **2**, 2089–2091.

MILES, J. W. & HENDERSON, D. 1990 *Ann. Rev. Fluid Mech.* **22**, 143–165.

NAYFEH, A. H. & MOOK, D. T. 1979 *Nonlinear Oscillations*. Wiley.

OTHMAN, A. M., WATT, D. & BARR, A. D. S. 1987 *J. Sound Vib.* **112**, 249–259.

PEARSON, J. R. A. 1959 *J. Fluid Mech.* **5**, 274–288.

PIERREHUMBERT, R. T. 1986 *Phys. Rev. Lett.* **57**, 2157–2159.

ROBINSON, A. C. & SAFFMAN, P. G. 1984 *J. Fluid Mech.* **142**, 451–466.

VLADIMIROV, V. A. 1983 *Prikl. Mech. Tekh. Fiz.* (no. 4), 39–61.

WALEFFE, F. 1990 *Phys. Fluids* A **2**, 76–80.